Initial results of Rayleigh scattering lidar observations at Zhongshan station, Antarctica

Ban Chao[1], Pan Weilin[1,2*], Wang Rui[3], Huang Wentao[3], Liu Fuchao[4],
Wang Zhangjun[5], Fang Xin[6], Cheng Xuewu[7], Hu Hongqiao[3]

(1. Key Laboratory of Middle Atmosphere and Global Environment Observation, Institute of Atmospheric Physics, Chinese Academy of Sciences, Beijing 100029, China;
2. University of Chinese Academy of Sciences, Beijing 100049, China;
3. Key Laboratory of Polar Science, Ministry of Natural Resources, Polar Research Institute of China, Shanghai 200136, China;
4. School of Electronic Information, Wuhan University, Wuhan 430072, China;
5. Institute of Oceanographic Instrumentation, Shandong Academy of Sciences, Qingdao 266100, China;
6. Key Laboratory of Geospace Environment, Chinese Academy of Sciences, University of Science and Technology of China, Hefei 230026, China;
7. Innovation Academy for Precision Measurement Science and Technology, Chinese Academy of Sciences, Wuhan 430071, China)

Abstract: A Rayleigh scattering lidar for measuring the atmospheric density and temperature has been deployed at Zhongshan Station (69.4° S, 76.4° E), Antarctica. Lidar transmitter was a frequency doubled Nd:YAG laser with ~400 mJ pulse energy and 30 Hz repetition rate. A telescope with 0.8 m diameter pointing to the zenith direction served as the lidar receiver. This lidar was capable of profiling the density and temperature in the Upper Stratosphere and Lower Mesosphere (USLM) region. At the vertical resolution of 300 m and the temporal resolution of 30 min, the lidar measurement uncertainties, mainly due to the photon noise, were calculated to be within 1.5% and 1 K for density and temperature, respectively. Since March 2020, this lidar has been routinely operated at Zhongshan station for exploring the atmospheric density and temperature variations and wave propagation characteristics in the polar USLM region.

Key words: Rayleigh scattering lidar; atmospheric density and temperature; Antarctica
CLC number: P356 **Document code:** A **DOI:** 10.3788/IRLA20210010

南极中山站瑞利散射激光雷达的初步探测结果

班 超[1], 潘蔚琳[1,2*], 王 睿[3], 黄文涛[3], 柳付超[4], 王章军[5], 方 欣[6], 程学武[7], 胡红桥[3]

(1. 中国科学院大气物理研究所 中层大气和全球环境探测重点实验室, 北京 100029;
2. 中国科学院大学, 北京 100049;
3. 中国极地研究中心 自然资源部极地科学重点实验室, 上海 200136;
4. 武汉大学 电子信息学院, 武汉 湖北 430072;
5. 山东省科学院海洋仪器仪表研究所, 青岛 山东 266100;
6. 中国科学技术大学 中国科学院近地空间环境重点实验室, 合肥 安徽 230026;
7. 中国科学院精密测量科学与技术创新研究院, 武汉 湖北 430071)

收稿日期:2020−12−20; **修订日期:**2021−02−05
基金项目:国家重点研发计划 (2016YFC1400300, 2018YFC1407301, 2018YFC1407305); 国家自然科学基金 (41904137); 中层大气和全球环境探测重点实验室开放课题 (LAGEO-2020-03)

摘　要：一套瑞利散射激光雷达已部署在南极中山站 (69.4° S, 76.4° E) 用于探测大气密度和温度。该激光雷达的光源为二倍频 Nd:YAG 脉冲激光器，重复频率 30 Hz，单脉冲能量约 400 mJ，同时使用一台 0.8 m 口径的垂直指向望远镜作为接收望远镜，可以探测平流层上层及中间层下层 (USLM) 区域的大气密度及温度廓线。在垂直分辨率为 300 m，时间分辨率为 30 min 的情况下，由光子噪声引起的大气密度和温度测量不确定性分别小于 1.5% 和 1 K。该激光雷达自 2020 年 3 月开始在中山站开展常规观测，有助于研究极区 USLM 区域的大气密度、温度的变化特征以及大气波动的传播特性。

关键词：瑞利散射激光雷达；　大气密度和温度；　南极

0 Introduction

The Upper Stratosphere and Lower Mesosphere (USLM) is an important region in the Earth's atmosphere. In this region, the amplitudes of atmospheric gravity waves (GW) and solar tides can be increased due to the decrease of air density with altitude[1]. When these waves propagate upwards, their energy and momentum can be deposited into the background and thereby modulate the atmosphere[2]. Long-term observations are important for studying the seasonal and inter-annual variability in the USLM region and for understanding global climate change[3−5]. Rayleigh scattering lidar has been proven an efficient means for making high-resolution measurements of density and temperature in the USLM region[5].

The first Rayleigh lidar observation of neutral density and temperature profiles was made by Hauchecorne and Chanin at the Haute-Provence Observatory[6]. Gardner et al. used a Rayleigh lidar to study the gravity waves characteristics at Urbana, Illinois[7]. Wichwar et al. used 3 years of Rayleigh lidar data at Logan, Utah to study the climatology of mesospheric temperature[8]. Recently, Llamedo et al. used an 11-year lidar temperature dataset at the altitudes of 20-56 km at Rio Gallegos, Argentina to study gravity wave activities and found that GW specific potential energy inside the polar vortex is larger than the outside or the edge of the vortex[5].

In the Antarctica region, Di Donfrancesco et al. used Rayleigh lidar observations to show an interesting temperature behavior and variation at McMurdo station (78° S, 167° E)[9]. Then Pan and Gardner combined Fe/Rayleigh lidar and high-altitude balloonsonde data to characterize the seasonal variations of atmospheric temperature from surface up to 110 km at South Pole[10]. Klekociuk et al. reported the seasonal variations of temperature in the stratosphere and lower mesosphere using the lidar data at Davis station (68.6° S, 78.0° E) near the Antarctica Circle[11]. Then Alexander et al. used Rayleigh lidar at Davis station to study the wintertime gravity wave activities in the USLM region[12]. Recently, Chu's group used 5 years (from 2011 to 2015) of lidar observation to characterize the GW between 30 km and 50 km at McMurdo station[3−4].

In China, Wu et al. firstly used a dual-beam Rayleigh lidar to obtain the air density and temperature profiles between 30 km and 43 km at Hefei[13]. After the system was upgraded, the lidar could measure the vertical distribution of atmospheric temperature from 22 km to 60 km[14]. From 2008, the Chinese meridian project deployed several lidars in China, including Rayleigh lidars at Beijing, Hefei, Wuhan, and Hainan[15]. Yue et al. used Rayleigh lidar data to analyze the middle atmosphere temperature structure at Beijing[16]. Qiao et al. and Dai et al. used a Rayleigh lidar measurements at Golmud, Qinghai to show the temperature and density profiles over the Tibetan Plateau region and analyzed the seasonal variations of atmospheric density[17−18].

The Rayleigh lidar presented in this paper is the first Rayleigh lidar deployed at Chinese stations in Antarctica. We will describe the lidar system configuration in Section 1, the data retrieval method in Section 2, our initial measurement results in Section 3, and then summarize in

the last Section.

1 Rayleigh lidar system

The Rayleigh lidar system at Zhongshan station consists of three units: laser transmitter, optical receiver, and time control & signal acquisition unit. Figure 1 shows lidar schematic diagram and the system configurations are listed in Tab.1.

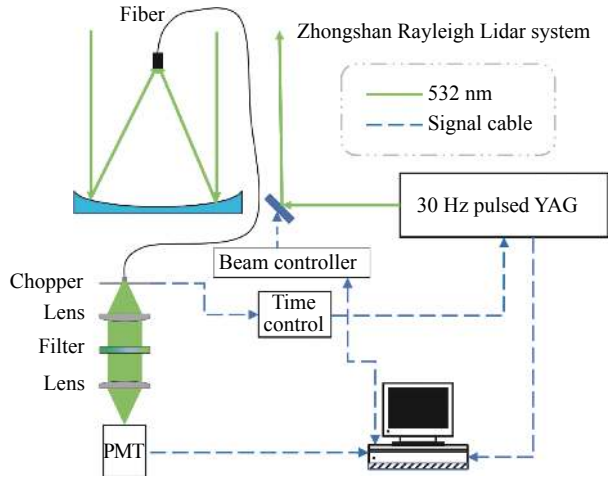

Fig.1 Schematic diagram of Zhongshan station Rayleigh lidar

Tab.1 System configurations of Zhongshan station Rayleigh lidar

Configuration	Parameters	
Laser transmitter	Wavelength/nm	532
	Pulse energy/mJ	400
	Repetition rate/Hz	30
	Pulse width/ns	8
Lidar receiver	Telescope diameter/m	0.8
	Telescope *f* number	1.8
	Fiber diameter/mm	1.5
	Fiber NA	0.39
	PMT quantum efficiency	~40% @ 532 nm
Time control & signal acquisition	Time generator	DG645
	Photon counting card	P7882

The lidar transmitter unit mainly consists of a neodymium-doped yttrium aluminum garnet (Nd:YAG) pulsed laser. The output laser is at the wavelength of 532 nm with single pulse energy ~400 mJ and repetition rate of 30 Hz. A high-precision beam controller is used to steer the laser beam to the zenith direction.

A prime focus telescope with the diameter of 0.8 m is used as lidar receiver. In order to perform well under the cold weather condition in Antarctica, the telescope's primary mirror was made of devitrified glass, which has relatively smaller thermal expansion coefficient. A multi-mode optical fiber with 1.5 mm core diameter and 0.39 numerical aperture (NA) is used to couple the telescope to the subsequent optical path. A mechanical chopper with the rotation rate of 5400 rpm is used to block the photon signal at lower altitudes for protecting the photon multiplier tube (PMT) from saturation. After passing through the chopper and an optical filter, received photons are finally detected by a PMT (Hamamatsu H7421-40, with the quantum efficiency ~40% at 532 nm).

The PMT converts optical photons to electrical signals being recorded by a digitizer (Fast ComTec MCA-3 Series/P7882). The timing control of the lidar is designed as follows. The primary timing is generated by the chopper in the receiving channel at the frequency of 180 Hz. Then the chopper triggers a digital delay/pulse generator (DG645) so that for every six pulses from the chopper, the DG645 is triggered once. Therefore a timing signal with the repetition rate of 30 Hz is produced to trigger the Nd:YAG laser's flash lamp. The same timing is also synchronized to the data acquisition unit.

2 Rayleigh lidar data retrieval method

The atmospheric density and temperature retrieval of Rayleigh lidar we used here follows a standard method[6], which is based on the lidar equation, ideal gas law, and hydrostatic equilibrium equation.

2.1 Density retrieval method

The Rayleigh scattering lidar equation can be expressed as:

$$N(z)=A\left(\eta T_{\mathrm{A}}^{2}\right)\left(\sigma_{\mathrm{ray}}\rho(z)\Delta z\right)\frac{1}{z^{2}}+N_{\mathrm{B}} \tag{1}$$

where A is a parameter dependent on both laser pulse energy and telescope diameter, η is system efficient, T_{A} is

atmospheric transmittance, σ_{ray} is Rayleigh backscatter cross section, $\rho(z)$ is atmospheric density at altitude z, and N_B is background noise. If we choose z_0 as the reference altitude, we can calculate atmospheric density at altitude z as:

$$\rho(z)=\frac{z^2(N(z)-N_B)}{z_0^2(N(z_0)-N_B)}\rho(z_0) \tag{2}$$

where $\rho(z)$ and $N(z)$ are the air density and lidar photon count at altitude z, respectively, $\rho(z_0)$ is the reference density from an atmospheric model. In our case, we used the MSIS (Mass Spectrometer and Incoherent Scatter) model[19–20].

The uncertainty of Rayleigh lidar density is caused by the random statistical uncertainty of PMT detected photon counts, which obeys the Poisson distribution, that is, $\Delta N(z)^2=N(z)$. Therefore, the uncertainty of Rayleigh lidar density can be expressed as:

$$\frac{\Delta\rho(z)}{\rho(z)}\approx\frac{\sqrt{N(z)}}{N(z)-N_B} \tag{3}$$

2.2 Temperature retrieval method

The ideal gas law is expressed as:

$$PV=nRT \tag{4}$$

where P is atmospheric pressure, V is volume, n is the amount of gas, R is the ideal gas constant, and T is temperature. The relation between mass and density can be expressed as:

$$\rho=\frac{m}{V} \tag{5}$$

And hydrostatic equilibrium equation is shown as:

$$\mathrm{d}P=-\rho g\mathrm{d}z \tag{6}$$

By combining Eq. (4)-(6), we can get the atmospheric temperature as:

$$T(z)=T(z_{seed})\frac{\rho(z_{seed})}{\rho(z)}+\frac{1}{R}\int_z^{z_{seed}}g(r)\mathrm{d}r\frac{\rho(r)}{\rho(z)} \tag{7}$$

where $T(z_{seed})$ and $\rho(z_{seed})$ are temperature and density at the seeding altitude z_{seed}, respectively. They are usually adopted from atmospheric model, such as the MSIS model.

To estimate the Rayleigh temperature uncertainty, Eq. (7) can be approximately expressed as:

$$T(z)\approx T(z_0)\left(\frac{z}{z_0}\right)^2\frac{N_R(z_0)}{N_R(z)}+\frac{\Delta z}{R}\sum_{r=z}^{z_0}\frac{N_R(r)}{N_R(z)}\frac{g(r)z^2}{r^2} \tag{8}$$

where $N_R(z)=N(z)-N_B$ is the Rayleigh scattering signal.

And from Eq. (8), the temperature uncertainty can be calculated as:

$$\Delta T(z)=\sum_{z_i=z+\Delta z}^{z_0}k(z_i)N(z_i)/$$
$$N(z)\sqrt{\frac{\sum_{z_i}k(z_i)^2\left(\overline{\Delta N(z_i)}\right)^2}{\left[\sum_{z_i}k(z_i)N(z_i)\right]^2}+\frac{\left(\overline{\Delta N(z_i)}\right)^2}{N(z_i)^2}} \tag{9}$$

where $k(z_i)=\frac{\Delta z}{R}g(z_i)\left(\frac{z_i}{z}\right)^2$ for $z_i=z+\Delta z,z+2\Delta z,\cdots,z_0$. Since the air density decreases exponentially with increasing altitude, the maximum temperature uncertainty is around the seeding altitude where the lidar signal is the weakest. From Eq. (9), the Rayleigh temperature uncertainty can be estimated by:

$$\Delta T(z)\leqslant T(z)*\sqrt{\frac{1+\frac{1}{SBR(z)}}{2N_R(z)}} \tag{10}$$

where $SBR(z)=N_R(z)/N_B$ is the signal to background ratio.

3 Lidar initial measurement results

A typical Rayleigh lidar raw signal profile at Zhongshan station is shown in Fig.2. This dataset was collected at 19:14:29 UT on March 6, 2020, with vertical resolution of 30 m and time resolution of 1 min (1 800 laser pulses at 30 Hz repetition rate). From Fig.2, we can

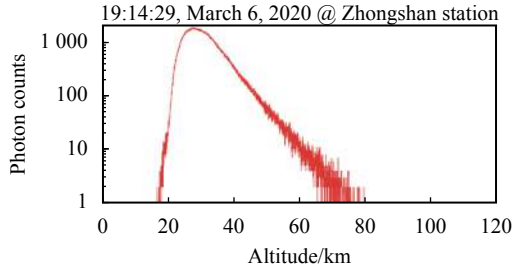

Fig.2 Rayleigh lidar raw signal profile at night on March 6, 2020, at Zhongshan station. The raw data has a vertical bin width of 30 m and an integration time of 1 min

see that the lidar signal below 17 km is fully blocked by the mechanical chopper. The transition for this chopper from fully close to fully open is about 15 km, so in our case we can use the lidar signal above 32 km for data retrieval. From 32 km to 60 km, the photon counts level decrease from ~1 000 to ~10. The background signal above 90 km is negligible, benefiting from less light pollution at night in the Antarctica region.

Using the retrieval method described in Section 2, we can calculate the atmosphere density and temperature profiles, shown in Fig. 3(a) and 3(c), respectively, with the vertical resolution of 300 m and temporal resolution of 30 min. The MSIS model results and the satellite measurements from the Sounding of Atmosphere Broadband Emission Radiometer (SABER)[21], onboard the Thermosphere Ionosphere and Mesosphere Electric Dynamics (TIMED) satellite, are used for lidar comparison. In general, we can see the atmospheric density and temperature profiles of lidar, MSIS, and SABER show a good agreement. The density in Fig.3(a) exponentially decays from 0.005 to ~0.000 2 kg/m^3 with increasing altitude. In Fig.3(c), all three results show that the temperature increases with altitude below stratopause and decreases with altitude above stratopause. Both lidar and

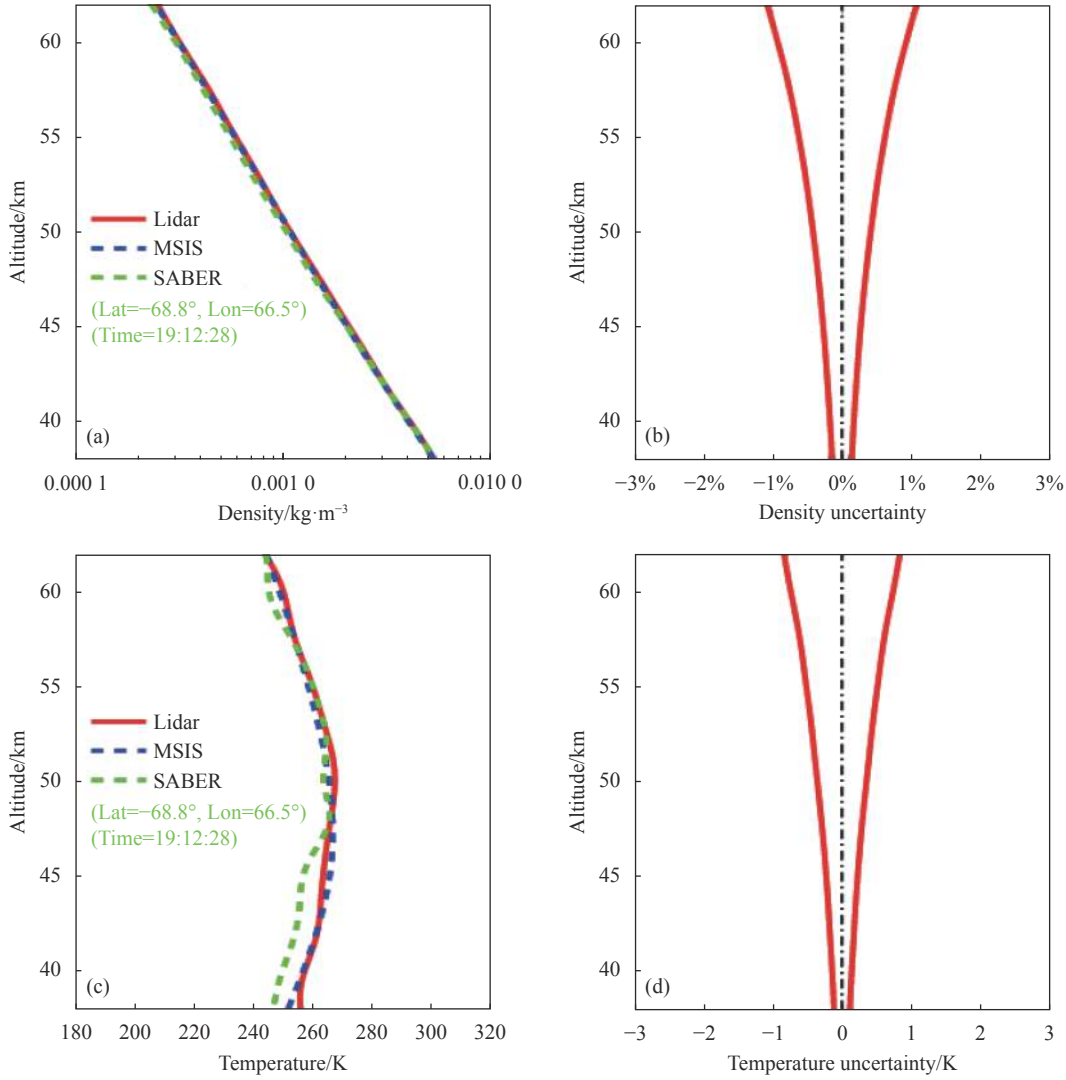

Fig.3 Comparison of atmospheric density (a) and temperature (c) between lidar (red solid), MSIS model (blue dash), and SABER satellite (green dash) data near Zhongshan station on March 6, 2020. The vertical resolution is 300 m and the temporal resolution is 30 min for lidar data. Lidar measured density uncertainty (b) and temperature uncertainty (d) were also plotted

SABER measurements exhibit more wave perturbation structures than the model. This may indicate that the MSIS model represents a mean status of atmosphere, but observations can reveal more details of the atmospheric wave information. Therefore lidar observations can be used to characterize the wave characteristics and to study how these waves influence the background atmosphere. Figure 3(b) and 3(d) are the lidar measurement uncertainties of density and temperature, respectively, based on the calculation of Eq.(3) and Eq.(10). The uncertainties shown here are mostly induced by lidar photon noise. We can see that the air density uncertainty is less than 1.5% and the temperature uncertainty is within 1 K.

Presented in Fig.4 are lidar observations lasting for ~10 h continuously on June 30, 2020, with 300 m vertical and 30 minutes temporal resolutions. From Fig.4(a), we can see that stratopause is around 52 km, and the stratopause temperature increases by almost 20 K from 265 K at 11∶15 UT to 285 K around 18∶15 UT, and then gradually decreases. The air density profiles, exponentially decreasing with increasing altitude, are shown in Fig.4(b) under the logarithm scale. In this case, the air density at 40 km is around 0.002 kg/m^3, and decreased with altitude to 5.0×10^{-5} kg/m^3 at 70 km. If we subtract the mean background temperature from the temperaturecolor contour in Fig.4(a), we can get the temperature perturbation in Fig.4(c), which shows wave structures of larger amplitude with increasing altitude. Similar method was applied to observe the atmospheric density and density perturbation. From Fig.4(c), we can estimate some wave parameters, such as the wave period of 6-7 hours, the vertical wavelength of 16-18 km, and the wave downward propagation speed of around 2.5 km/h. And in Fig.4(d), similar wave structure is also shown in density perturbation plot. Overall, the temperature and

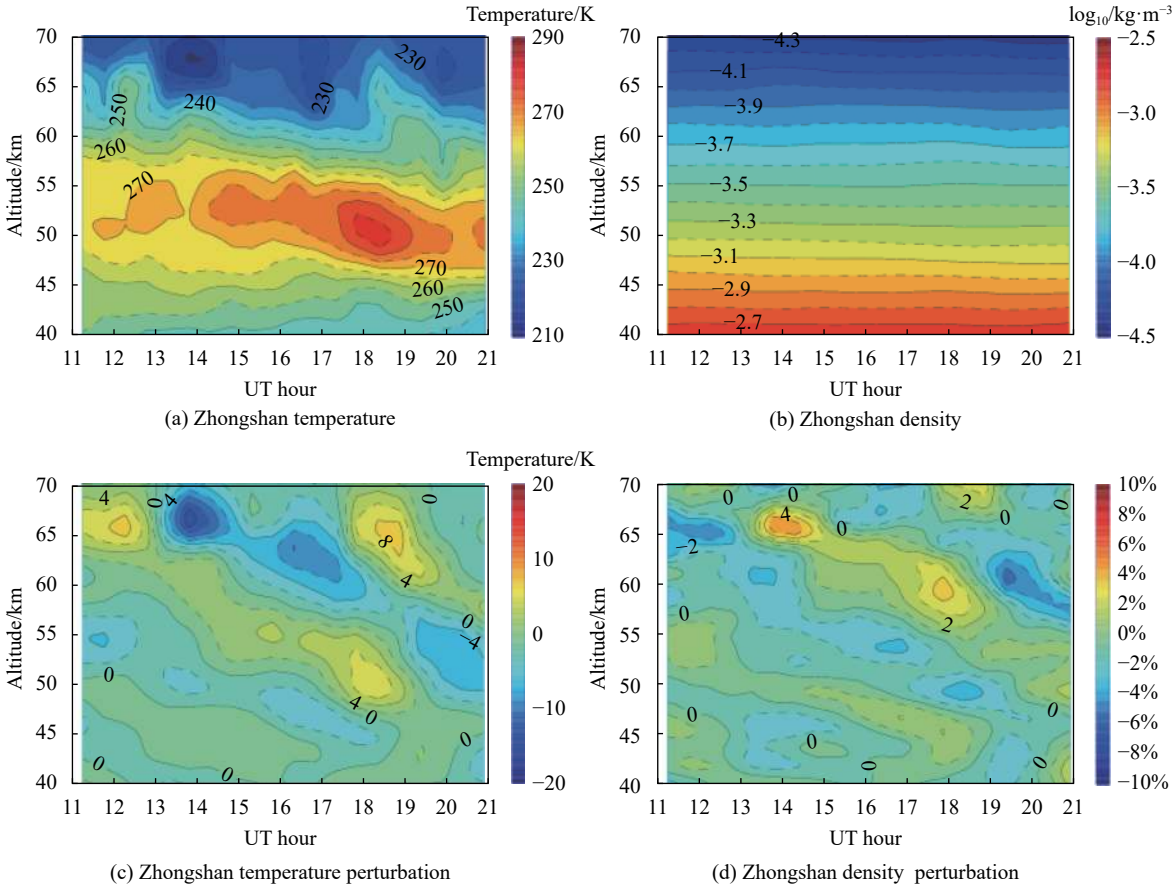

Fig.4 Zhongshan station Rayleigh lidar measured temperature (a), density (b), temperature perturbation (c), and density perturbation (d) on June 30, 2020. The density (b) is plotted in color contour under the logarithm scale

density perturbations presented here demonstrate that the Zhongshan station Rayleigh lidar is capable of providing high-resolution dataset for investigating the middle atmosphere waves in the Antarctica region.

4 Conclusion

A Rayleigh lidar has been deployed at Zhongshan station (69.4° S, 76.4° E), Antarctica, and operated since March 2020. Using a 400 mJ laser and 0.8 m diameter primary focus telescope, atmospheric density and temperature were measured in the USLM region. The lidar measured density and temperature profiles on March 6, 2020 are presented. A comparison of lidar, MSIS model, and satellite (SABER/TIMED) result shows a good agreement. Lidar measurement uncertainties of density and temperature were mostly induced by photon noise. At nighttime under clear sky condition, the density uncertainty is less than 1.5% and the temperature uncertainty is less than 1.0 K. A continuous observation on June 30, 2020 showed wave structure in the middle atmosphere at Zhongshan station. Thus, this lidar can provide a reliable dataset for studying USLM thermal structure, waves, and energy exchange among different atmospheric layers. We also plan to upgrade the lidar system by extending the altitude coverage.

References:

[1] Fritts D C, Alexander M J. Gravity wave dynamics and effects in the middle atmosphere [J]. ***Reviews of Geophysics***, 2003, 41(1): 1003.

[2] Ban C, Li T, Fang X, et al. Sodium lidar-observed gravity wave breaking followed by an upward propagation of sporadic sodium layer over Hefei, China [J]. ***Journal of Geophysical Research*: *Space Physics***, 2015, 120: 7958-7969.

[3] Zhao J, Chu X Z, Chen C, et al. Lidar observations of stratospheric gravity waves from 2011 to 2015 at McMurdo (77.84° S, 166.69° E), Antarctica: 1. Vertical wavelengths, periods, and frequency and vertical wave number spectra [J]. ***Journal of Geophysical Research*: *Atmospheres***, 2017, 122: 5041-5062.

[4] Chu X Z, Zhao J, Lu X, et al. Lidar observations of stratospheric gravity waves from 2011 to 2015 at McMurdo (77.84° S, 166.69° E), Antarctica: Part II. Potential energy densities, lognormal distributions, and seasonal variations [J]. ***Journal of Geophysical Research*: *Atmospheres***, 2018, 123: 7910-7934.

[5] Llamedo P, Salvador J, Torre A de la, et al. 11 years of Rayleigh lidar observations of gravity wave activity above the southern tip of South America [J]. ***Journal of Geophysical Research*: *Atmospheres***, 2019, 124: 451-467.

[6] Hauchecorne A, Chanin M L. Density and temperature profiles obtained by Lidar between 35 km and 70 km [J]. ***Geophysical Research Letters***, 1980, 7(8): 565-568.

[7] Gardner C S, Miller M S, Liu C H. Rayleigh lidar observations of gravity wave activity in the upper stratosphere at Urbana, Illinois [J]. ***Journal of the Atmospheric Sciences***, 1988, 46(12): 1838-1854.

[8] Wickwar V B, Beissner K C, Wilkerson T D, et al. Climatology of Mesospheric Temperature Profiles Observed with the Consortium Rayleigh-Scatter Lidar at Logan, Utah[M]// Ansmann A, Neuber R, Rairoux P, et al. Advances in Atmospheric Remote Sensing with Lidar. Berlin, Heidelberg, New York: Springer, 1997.

[9] Di Donfrancesco G, Adriani A, Gobbi G P, et al. Lidar observations of stratospheric temperature above McMurdo station, Antarctica [J]. ***Journal of Atmospheric and Terrestrial Physics***, 1996, 58: 1391-1399.

[10] Pan W, Gardner C S. Seasonal variations of the atmospheric temperature structure at South Pole [J]. ***Journal of Geophysical Research Atmospheres***, 2003, 108: 4564.

[11] Klekociuk A R, Lambert M M, Vincent R A, et al. First year of Rayleigh lidar mearsurements of middle atmosphere temperature above Davis, Antarctica [J]. ***Advances in Space Research***, 2003, 32: 771-776.

[12] Alexander S P, Klekociuk A R, Murphy D J. Rayleigh lidar observations of gravity wave ativity in the winter upper stratosphere and lower mesosphere above Davis, Antarctica (69° S, 78° E) [J]. ***Journal of Geophysical Research*: *Atmospheres***, 2011, 116: D13109.

[13] Wu Y H, Hu H L, Hu S X, et al. Atmospheric density and temperature measurement with lidar in the middle and upper stratosphere [J]. ***Chinese Journal of Quantum Electronics***, 2000, 17(5): 426-431.

[14] Wu Y H, Hu H L, Hu S X, et al. Measurements of thermal profiles in the stratosphere and lower mesosphere with Rayleigh scattering lidar [J]. ***Chinese Journal of Atmospheric Sciences***, 2002, 26(1): 23-29. (in Chinese)

[15] Wang C. New chains of space weather monitoring stations in China [J]. ***Space Weather***, 2010(8): S08001.

[16] Yue C, Yang G, Wang J, et al. Lidar observations of the middle atmospheric thermal structure over north China and comparisons with TIMED/SABER [J]. ***Journal of Atmospheric and Solar-Terrestrial Physics***, 2014, 120(1): 80-87.

[17] Qiao S, Pan W, Zhu K Y, et al. Initial results of lidar measured middle atmosphere temperatures over Tibetan Plateau [J]. ***Atmospheric and Oceanic Science Letters***, 2014, 7(3): 213-217.

[18] Dai Y, Pan W, Qiao S, et al. Seasonal variations of middle atmosphere densities observed by Rayleigh lidar at Golmud, Qinghai [J]. ***Chinese Journal of Space Science***, 2020, 40(2): 207-214.

[19] Hedin A E. Extension of the MSIS thermosphere model into the middle and lower atmosphere [J]. ***Journal of Geophysical Research: Space Physics***, 1991, 96: 1159-1172.

[20] Picone J M, Hedin A E, Drob D P, et al. NRLMSISE-00 empirical model of the atmosphere: Statisticalcomparisons and scientific issues [J]. ***Journal of Geophysical Research: Space Physics***, 2002, 107(A12): 1468.

[21] Russell J M III, Mlynczak M G, Gordley L L, et al. An overview of the SABER experiment and preliminary calibration results[C]//Proc of SPIE, 1999, 3756: 277- 288.

第一作者简介： 班超 (1988−), 男, 博士后, 博士。主要从事大气遥感探测技术及中高层大气动力学研究。参与研制青藏高原首台臭氧探测激光雷达、南极首台三方向钠荧光多普勒激光雷达等先进探测设备。作为项目负责人主持国家科学自然基金, 参与重点研发计划、中国科学院战略性科技先导专项等多个项目。Email: banchao@mail.iap.ac.cn

通讯作者简介： 潘蔚琳 (1973−), 研究员级高级工程师, 博士生导师, 博士。主要从事大气光学遥感探测研究。1998~2002 年参与研制国际首台铁玻尔兹曼激光雷达, 并应用于南、北极中层大气探测研究。2013 年利用自主研发的瑞利激光雷达在青藏高原首次开展中高层大气温度的地基探测研究, 2012~2017 年承担基金委国家重大科研仪器设备研制专项“多波段多大气成分主被动组合探测系统 (APSOS)”课题二“气溶胶-云-水汽探测激光雷达”, 并负责 APSOS 系统在西藏羊八井的部署实施。2003 年美国光学学会 (OSA) 的 Allen Prize 获得者。目前担任中国科学院日地空间网科学委员会 (STERN) 委员。Email: panweilin@mail.iap.ac.cn